Location Optimization for RIS aided mmWave downlink network

Qian Xiang, **Cong Sun**, Danpu Liu, Beijing University of Posts and Telecommunications
suncong86@bupt.edu.cn

INTRODUCTION

- **Reconfigurable Intelligent Surface (RIS)**: passive phase shift; high energy efficiency; popular candidate technique for 6G
- **Millimeter wave (mmWave)**: short wavelength; wide frequency band; great directivity

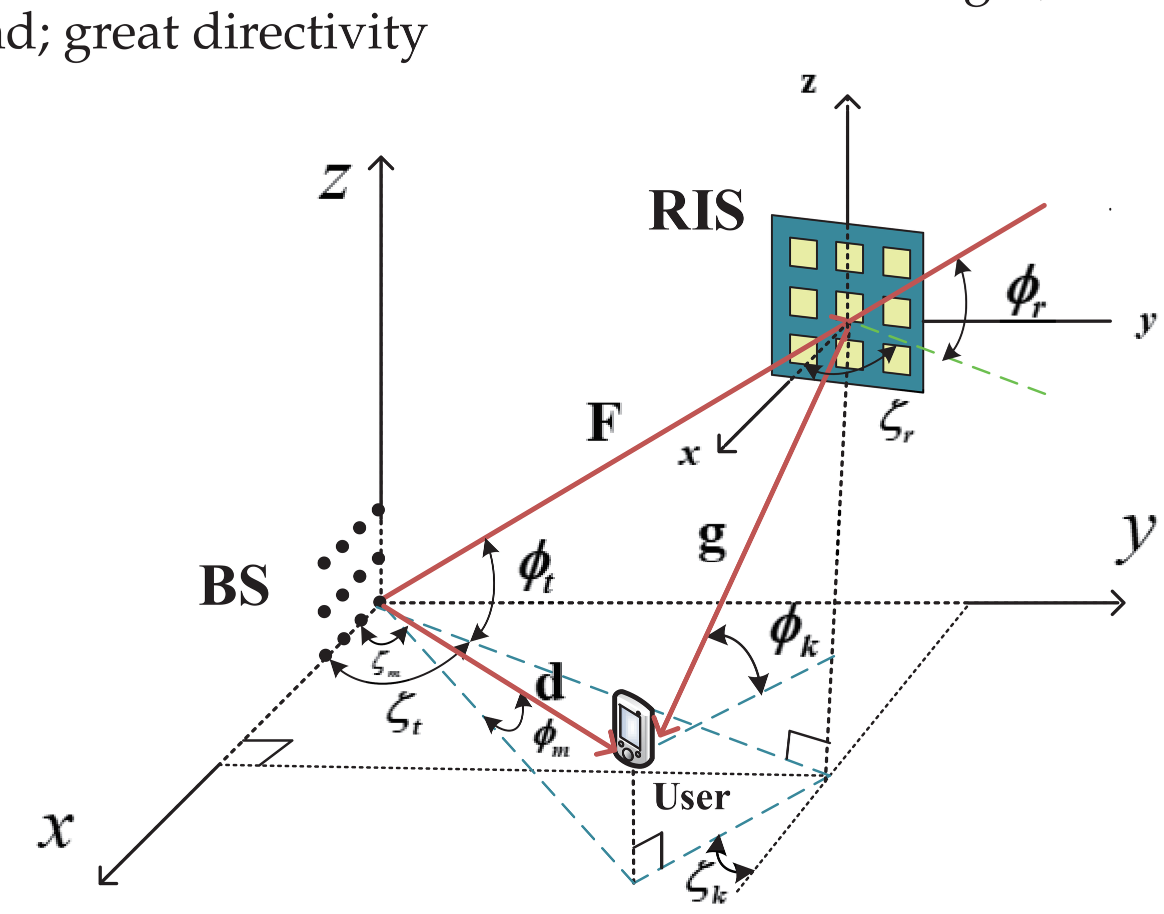

SYSTEM MODEL

Saleh-Valenzuela (SV) channels for UPAs at BS and RIS:

$$\mathbf{F}{=}L(l_B)\mathbf{a}_R(\zeta_r,\phi_r)\mathbf{a}_T(\zeta_t,\phi_t)^H,\ \mathbf{g}{=}L(l_U)\mathbf{a}_R(\zeta_k,\phi_k),\ \mathbf{d}{=}L(l_d)\mathbf{a}_T(\zeta_m,\phi_m),$$

where the path loss component, the normalized receive and transmit array response vector (ARV) are as follows respectively:

$$L(l_B) = C(\frac{l_B}{l_0})^{-\alpha},$$

$$\mathbf{a}_R(\zeta_r,\phi_r)=\left[1,\dots,e^{j\frac{2\pi d_R}{\lambda}(N_x-1)\sin\zeta_r\sin\phi_r}\right]^T\otimes\left[1,\dots,e^{j\frac{2\pi d_R}{\lambda}(N_z-1)\cos\phi_r}\right]^T,$$

$$\mathbf{a}_T(\zeta_t,\phi_t)=\left[1,\dots,e^{j\frac{2\pi d_B}{\lambda}(M_x-1)\sin\zeta_t\sin\phi_t}\right]^T\otimes\left[1,\dots,e^{j\frac{2\pi d_B}{\lambda}(M_z-1)\cos\phi_t}\right]^T.$$

Here $\mathbf{r}=(x_r,y_r,z_r)^T$ represents the location of RIS, $\sin\zeta_r=\frac{y_r}{\|(\mathbf{b}-\mathbf{r})_{1,2}\|}$, $\sin\phi_r=\frac{z_r-z_b}{\|\mathbf{r}-\mathbf{b}\|}$, $\zeta_t=\zeta_r$ and $\phi_t=\phi_r$.

The signal received at the user is:

$$y=\left(\mathbf{d}^H+\mathbf{g}^H\mathbf{\Theta}\mathbf{F}\right)\mathbf{w}s+n,$$

where $n\sim\mathcal{CN}(0,\sigma^2)$, s is the transmit signal for the user satisfying $\mathbb{E}(|s|^2)=1$, $\mathbf{w}\in\mathbb{C}^M$ is the precoding vector and $\mathbf{\Theta}=\mathrm{Diag}(\theta_1,\dots,\theta_N)$ is the RIS matrix.

SNR MAXIMIZATION

$$\max_{\substack{\mathbf{w}\in\mathbb{C}^M,\mathbf{r}\in R^3,\\ \mathbf{\Theta}\in\mathbb{C}^{N\times N}}}\ \mathrm{SNR}=\frac{|(\mathbf{d}^H+\mathbf{g}(\mathbf{r})^H\mathbf{\Theta}\mathbf{F}(\mathbf{r}))\mathbf{w}|^2}{\sigma^2}$$
$$\text{s. t.}\quad \|\mathbf{w}\|^2\le P_T,\qquad\qquad (1)$$
$$\mathbf{\Theta}=\mathrm{Diag}(\theta_1,\dots,\theta_N),\theta_l\in\Omega,l=1,\dots,N.$$

RIS constraint:

$$\Omega=\left\{e^{i\varphi},\varphi\in\left\{0,\frac{2\pi}{T},\cdots,\frac{2\pi(T-1)}{T}\right\}\right\}\ \text{or}\ \{\theta_l\in\mathbb{C}\mid|\theta_l|\le1\}.$$

Plug the optimal MRT precoding vector $\mathbf{w}^*=\frac{\sqrt{P_T}}{\|\mathbf{h}\|}\mathbf{h}$ into (1), and the equivalent optimization problem becomes:

$$\max_{\mathbf{v}\in\mathbb{C}^N,\mathbf{r}\in R^3}\ \|\mathbf{h}(\mathbf{v},\mathbf{r})\|^2\qquad\qquad (2)$$
$$\text{s. t.}\quad \theta_l\in\Omega,l=1,\dots,N,$$

where $\mathbf{h}(\mathbf{v},\mathbf{r})=\mathbf{d}+\mathbf{F}^H\mathbf{\Theta}^H\mathbf{g}$

$$=\mathbf{d}+\frac{C^2}{\|\mathbf{u}-\mathbf{r}\|^2\|\mathbf{b}-\mathbf{r}\|^2}\left[\mathbf{a}_R(\zeta_r(\mathbf{r}),\phi_r(\mathbf{r}))^H\mathbf{B}\mathbf{v}\right]\mathbf{a}_T(\zeta_t(\mathbf{r}),\phi_t(\mathbf{r})).$$

Here $\mathbf{v}=(\theta_1,\dots,\theta_N)^H$, and $\mathbf{B}=\mathrm{Diag}\left[\mathbf{a}_R(\zeta_k(\mathbf{r}),\phi_k(\mathbf{r}))\right]$.

ADMM METHOD

Augmented Lagrangian penalty function technique:

$$\begin{aligned}\max_{\mathbf{v},\mathbf{r},\mathbf{p}}\ &\|\mathbf{h}(\mathbf{v},\mathbf{r})\|^2\\ \text{s. t.}\ &\mathbf{p}=\mathbf{v},\\ &p_l\in\Omega,l=1,\dots,N.\end{aligned}\quad\Rightarrow\quad\begin{aligned}\min_{\mathbf{v},\mathbf{r},\mathbf{p}}\ &-\|\mathbf{h}(\mathbf{v},\mathbf{r})\|^2+\mathrm{Re}\left\{\boldsymbol{\mu}^H(\mathbf{p}-\mathbf{v})\right\}\\ &+\frac{\rho}{2}\|\mathbf{p}-\mathbf{v}\|^2\\ \text{s. t.}\ &p_l\in\Omega,l=1,\dots,N.\end{aligned}$$

- $\mathbf{v}$ subproblem: $\min_{\mathbf{v}}\frac{1}{2}\mathbf{v}^H\mathbf{Q}\mathbf{v}+\mathrm{Re}(\mathbf{v}^H\mathbf{q})$
  closed-form solution: $\mathbf{v}_{k+1}=-\mathbf{Q}^{-1}\mathbf{q}$, or
  solution with sufficient function reduction: $\mathbf{v}_{k+1}=\mathbf{v}_k+\alpha_k\mathbf{d}_k$.
- $\mathbf{p}$ subproblem:

$$\begin{aligned}\min_{\mathbf{p}\in\mathbb{C}^N}\ &\frac{\rho}{2}\mathbf{p}^H\mathbf{p}+\mathrm{Re}\{(\boldsymbol{\mu}-\rho\mathbf{v})^H\mathbf{p}\}\\ \text{s. t.}\ &p_l\in\Omega,l=1,\dots,N.\end{aligned}\ \overset{\text{closed-form}}{\underset{\text{solution}}{\Rightarrow}}\ p_l^*=\begin{cases}\eta_l, & \text{if } |\eta_l|\le1,\\ \frac{\eta_l}{|\eta_l|}, & \text{otherwise.}\end{cases}$$

$$\text{or } p_l^*=e^{i\varphi_l^*},\varphi_l^*=\mathop{\arg\min}_{\varphi_l\in\left\{0,\frac{2\pi}{T},\cdots,\frac{2\pi(T-1)}{T}\right\}}|\varphi_l-\mathrm{Arg}(\rho\eta_l)|,\ \eta_l=v_l-\frac{\mu_l}{\rho}.$$

- $\mathbf{r}$ subproblem: $\min_{\mathbf{r}}\ -\|\mathbf{h}(\mathbf{v},\mathbf{r})\|^2$
  Levenberg-Marquardt (LM) method:

$$\mathbf{r}^{k+1}=\mathbf{r}^k+\left(\gamma_k\mathbf{I}-\mathrm{Re}\{\mathbf{J}_k^H\mathbf{J}_k\}\right)^{-1}\mathrm{Re}\{\mathbf{J}_k^H\mathbf{h}_k\},$$

  from subproblem:

$$\min_{\mathbf{r}}\ -\left\|\mathbf{h}(\mathbf{r})+\mathbf{J}(\mathbf{r}^k)(\mathbf{r}-\mathbf{r}^k)\right\|^2\ \text{s. t. }\|\mathbf{r}-\mathbf{r}^k\|\le\Delta_k.$$

SIMULATION RESULTS

Parameter settings: $\mathbf{b}=(0,0,10)^T$, $\mathbf{u}=(50,50,5)^T$, $M_x=4$, $M_z=4$, $N_x=10$, $N_z=\frac{N}{N_x}$, $\sigma^2=-110$dBm, $P_T=2.5$dBm, $T=4$.

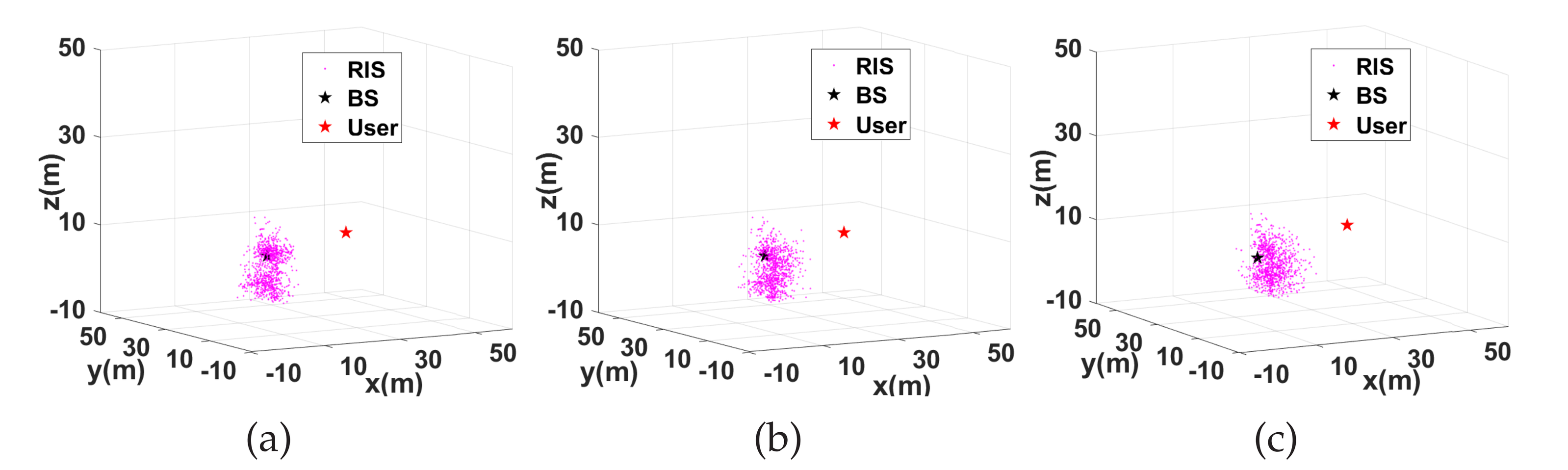

Figure 1: RIS locations with different initial setting

The initial RIS location $\mathbf{r}^0$ is randomly selected from the 10m radius circle centered at: (a) BS; (b) midpoint between BS and the user; (c) the user.

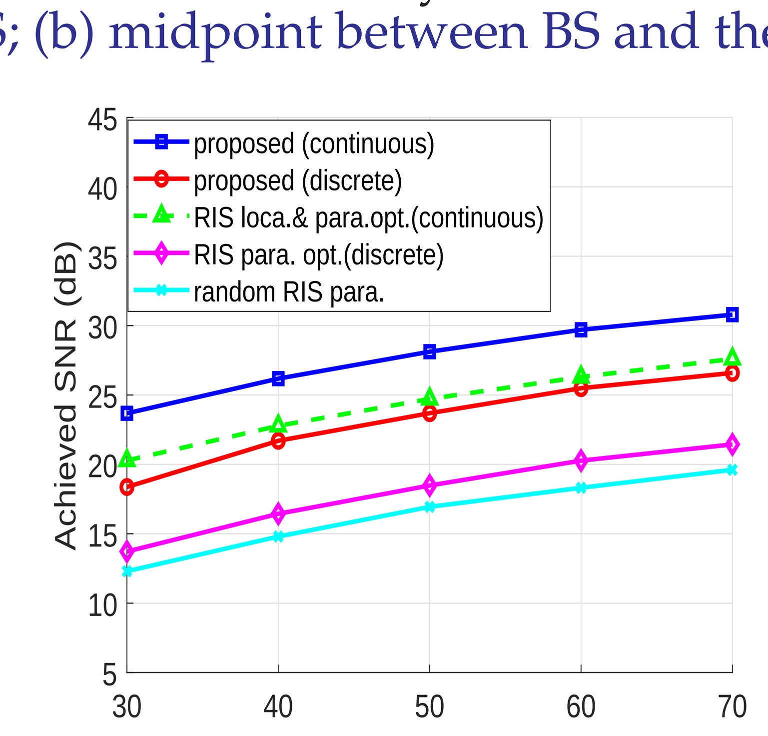

Figure 2: Achieved SNR with respect to N

Joint optimization of RIS location and parameters greatly outperforms other benchmarks.

REFERENCES

[1] H. Lu, Y. Zeng, S. Jin and R. Zhang, "Aerial Intelligent Reflecting Surface: Joint Placement and Passive Beamforming Design With 3D Beam Flattening," IEEE Transactions on Wireless Communications, vol. 20, no. 7, pp. 4128-4143, July 2021.

[2] Q. Wu and R. Zhang, "Beamforming Optimization for Intelligent Reflecting Surface with Discrete Phase Shifts," IEEE International Conference on Acoustics, Speech and Signal Processing (ICASSP), pp. 7830-7833, Apr. 2019.